A novel system to map protein interactions reveals evolutionarily conserved immune evasion pathways on transmissible cancers

Flies, A.S.; Darby, J.M.; Lennard, P.R.; Murphy, P.R.; Ong, C.E.B.; Pinfold, T.L.; ... ; Patchett, A.L.

CANCER

A novel system to map protein interactions reveals evolutionarily conserved immune evasion pathways on transmissible cancers

Andrew S. Flies[1]*, Jocelyn M. Darby[1], Patrick R. Lennard[1,2†], Peter R. Murphy[1,3†], Chrissie E. B. Ong[1], Terry L. Pinfold[4], Alana De Luca[4], A. Bruce Lyons[4], Gregory M. Woods[1], Amanda L. Patchett[1]

Around 40% of humans and Tasmanian devils (*Sarcophilus harrisii*) develop cancer in their lifetime, compared to less than 10% for most species. In addition, devils are affected by two of the three known transmissible cancers in mammals. Immune checkpoint immunotherapy has transformed human medicine, but a lack of species-specific reagents has limited checkpoint immunology in most species. We developed a cut-and-paste reagent development system and used the fluorescent fusion protein system to show that immune checkpoint interactions are conserved across 160,000,000 years of evolution, CD200 is highly expressed on transmissible tumor cells, and coexpression of CD200R1 can block CD200 surface expression. The system's versatility across species was demonstrated by fusing a fluorescent reporter to a camelid-derived nanobody that binds human programmed death ligand 1. The evolutionarily conserved pathways suggest that naturally occurring cancers in devils and other species can be used to advance our understanding of cancer and immunological tolerance.

INTRODUCTION

Metastatic cancer affects most mammals, but the cancer incidence can vary widely across phylogenetic groups and species (Fig. 1 and table S1) (*1*–*3*). In humans, the lifetime risk of developing cancer is around 40% (*4*). This figure is in stark contrast to a general cancer incidence of 3% for mammals, 2% for birds, and 2% for reptiles reported by the San Diego Zoo (N = 10,317) (*2*, *5*). A more recent study at the Taipei Zoo reported cancer incidence of 8, 4, and 1% for mammals, birds, and reptiles, respectively (N = 2657) (*6*). Cancer incidence in domestic animals is generally less than 10% (N = 202,277) (*3*). However, two studies performed 40 years apart reported that greater than 40% of Tasmanian devils develop spontaneous, often severe neoplasia in their lifetime (*5*, *7*). Devils are also unique because they are affected by two of the three known naturally occurring transmissible cancers in vertebrate species (*8*, *9*). Transmissible cancers are a distinct form of cancer in which the tumor cells function as an infectious pathogen and an allograft. Dogs (*Canis lupus familiaris*) are the only other vertebrate species affected by a transmissible cancer (*10*), and interestingly, some breeds of dogs also have high cancer incidence (*3*, *11*).

The devil facial tumor (DFT) disease was first detected in Northwest Tasmania and has been a primary driver of an 80% decline in the wild Tasmanian devil population (*8*, *12*). The clonal DFT (DFT1) cells have been continually transmitted among devils and are estimated to have killed at least 10,000 individuals since at least 1996. In 2014, a second independent transmissible Tasmanian DFT (DFT2) was found in wild devils (*9*), and 23 cases have been reported to date (*13*). Genetic mismatches, particularly in the major histocompatibility complex (MHC) genes, should lead to rejection of these transmissible tumors. Consequently, the role of devil MHC has been a focus of numerous studies (Fig. 1 and table S1) to understand the lack of rejection of the transmissible tumors. These studies have revealed that the DFT1 cells down-regulate MHC class I (MHC-I) expression (*14*), a phenomenon observed in many human cancers. In contrast to DFT1 cells, the DFT2 cells do express MHC-I (*15*). DFT1 and DFT2 cells have 2884 and 3591 single-nucleotide variants, respectively,

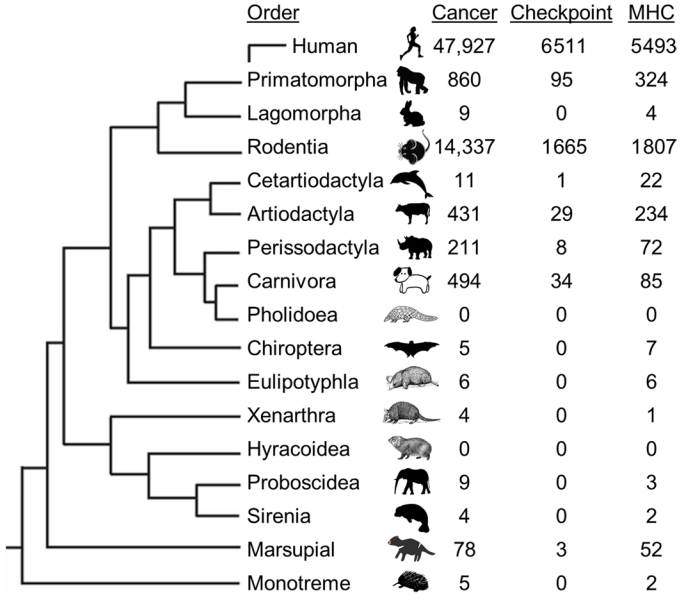

Fig. 1. Phylogenetic tree of immune system–related studies in mammal orders from 2009 to 2019. Metastatic cancer has been reported in nearly all mammalian orders, and MHCs have been the most intensely studied molecules in most orders. In the past decade, studies of immune checkpoint molecules (PD1, PDL1, and CTLA4) have become a primary focus in humans and rodents. However, immune checkpoint studies in other species are limited, particularly at the protein level, because of the lack of species-specific reagents. This creates a vast gap in our understanding of the evolution of the mammalian immune system. The numbers in the columns represent the number studies matching Web of Science search results between 2009 and 2019. See table S1 for search terms.

[1]Menzies Institute for Medical Research, College of Health and Medicine, University of Tasmania, Hobart, TAS 7000, Australia. [2]The Roslin Institute and Royal School of Veterinary Studies, University of Edinburgh, Easter Bush Campus, Midlothian EH25 9RG, UK. [3]University of Queensland Diamantina Institute, The University of Queensland, Translational Research Institute, Woolloongabba, QLD, Australia. [4]School of Medicine, College of Health and Medicine, University of Tasmania, Hobart, TAS 7000, Australia.
*Corresponding author. Email: andy.flies@utas.edu.au
†Present Address: Menzies Institute for Medical Research College of Health and Medicine University of Tasmania Private Bag 23, Hobart TAS 7000, Australia.

that are not present in 46 normal devil genomes (*16*). The continual transmission of DFT1 and DFT2, despite MHC-I expression by DFT2 cells and genetic mismatches between host and tumor, suggests that additional pathways are likely involved in immune evasion.

Human cancer treatment has been transformed in the past decade by manipulating interactions among immune checkpoint molecules. These have proven broadly effective in part because they function across many different MHC types and tumor mutational patterns. However, these pathways have received little attention in transmissible cancers and other naturally occurring cancers in nonmodel species (Fig. 1 and table S1) (*17*–*19*). We have previously shown that the inhibitory immune checkpoint molecule programmed death ligand 1 (PDL1) is expressed in the DFT microenvironment and is up-regulated by interferon-γ (IFN-γ) in vitro (*17*). This finding led us to question which other immune checkpoint molecules play a role in immune evasion by the transmissible cancers and the devil's high spontaneous cancer incidence. Understanding immune evasion in a natural environment will support DFT vaccine development to help protect this endangered species (*20*) and has the potential to identify protein interactions that are conserved across divergent species to improve translational success of animal models (*19*). Unfortunately, a persistent limitation for immunology in nontraditional study species is a lack of species-specific reagents. Wildlife biologists and veterinarians are at the front lines of emerging infectious disease outbreaks, but they often lack species-specific reagents to fulfill the World Health Organization's call for "cross-cutting R&D preparedness" and perform mechanistic immunological investigations.

To solve the paucity of reagents available for Tasmanian devils and address ongoing limitations for nontraditional study species, we developed a Fluorescent Adaptable Simple Theranostic (FAST) protein system that builds on the diverse uses of fluorescent proteins previously reported (*21*–*23*). This simple system can be used for rapid development of diagnostic and therapeutic (i.e., theranostic) immunological toolkits for any animal species (Fig. 2). We demonstrate the impact of the FAST system by using it to confirm seven receptor-ligand interactions among 12 checkpoint proteins in devils. We demonstrate the versatility of the system across species by fusing a fluorescent reporter to a well-characterized camelid-derived nanobody that binds human PDL1 (*24*).

In humans, checkpoint proteins have been targets of immunotherapy in clinical trials, but the functional role and binding patterns of these proteins are unknown for most other species. We have used the FAST system to show that the inhibitory checkpoint protein CD200 is highly expressed on DFT cells, opening the door to single-cell phenotyping of circulating tumor cells (CTCs) in devil blood. Furthermore, we are the first to report that coexpression of CD200R1 can block surface expression of CD200 in any species. Understanding how clonal tumor cells graft onto new hosts, evade immune defenses and metastasize within a host will identify evolutionarily conserved immunological mechanisms to help improve cancer, infectious disease, and transplant outcomes for human and veterinary medicine.

RESULTS

Fluorescent fusion proteins can be secreted from mammalian cells

Initially, we developed FAST proteins to determine whether monomeric fluorescent proteins could be fused to devil proteins and secreted from mammalian cells (Fig. 2A and table S2). We used 41BB (TNFRSF9) for proof-of-concept studies by fusing the extracellular domain of devil 41BB checkpoint molecule to monomeric fluorescent proteins (Fig. 2, A and B, and fig. S1). We used wild-type Chinese hamster ovary (CHO) cells and CHO cells transfected with 41BBL (TNFSF9) to confirm specificity of the 41BB FAST proteins and demonstrate that the fluorescent proteins [mTag-blue fluorescent protein (BFP), mCerulean3, mAzurite, mCitrine, mOrange, mCherry, and mNeptune2] remained fluorescent when secreted from mammalian cells (Fig. 2C).

We chose mCherry, mCitrine, mOrange, and mBFP for ongoing FAST protein development. Initial batches of FAST proteins were purified using the 6xHis tag and eluted with imidazole. Following purification of FAST protein the color can be immediately observed with blue light and an amber filter unit, allowing confirmation that the fluorescent protein DNA coding sequences were in frame and the proteins were properly folded. After combining, concentrating, and sterile filtering the eluted fractions, 100 µl at 1 mg/ml was aliquoted and visualized again using blue light to confirm fluorescent signal (Fig. 2B). A full step-by-step protocol and set of experimental templates for creating and testing FAST proteins for any species are available online in the Supplementary Materials.

Receptor-ligand binding confirmed in single-step staining assays

We chose candidate immune checkpoint molecules for FAST protein development (Fig. 3A and table S2) based on targets of human clinical trials and then selected devil genes for which a reliable sequence was available either in the published devil genome or transcriptomes (*19*, *25*, *26*). We transfected the FAST protein expression vectors (table S3) into CHO cells and tested the supernatant against CHO cell lines expressing full-length receptors. 41BB FAST proteins in supernatant exhibited strong binding to 41BBL cell lines, but the fluorescent signals from most other FAST proteins were too weak to confirm binding to the expected receptors (fig. S2). As FAST proteins do not require secondary reagents, we next incubated target cells with purified FAST proteins and added chloroquine to block the lysosomal protein degradation pathway. This allowed us to take advantage of receptor-mediated endocytosis, which can allow accumulation of captured fluorescent signals inside the target cells (*27*). This protocol adjustment allowed confirmation that CD47-mCherry, CD200-mBFP, CD200-mOrange, CD200R1-mBFP, and CD200R1-mOrange, and PD1-mCitrine bound to their expected receptors (Fig. 3B). We also demonstrated the flexibility of the FAST proteins by showing that alternative fusion conformations (fig. S1, C and D), such as type II proteins (e.g., mCherry-41BBL) and a devil Fc tag (e.g., CD80-Fc-mCherry) bound to their expected ligands (Fig. 3B). The stability of the fusion proteins was demonstrated using supernatants that were stored at 4°C for 2 months before use in a 1-hour live-culture assay with chloroquine (fig. S3).

Cell lines secreting FAST proteins confirm protein interactions in live coculture assays

To further streamline the reagent development process, we next took advantage of the single-step nature of FAST proteins (i.e., no secondary antibodies or labels needed) in live-cell coculture assays (Fig. 4A). Cell lines secreting 41BB-mCherry, 41BBL-mCherry, or CD80-Fc-mCherry FAST proteins were mixed with cell lines expressing full-length 41BB, 41BBL, or CTLA4-mCitrine and cocultured at a 1:1 ratio overnight with chloroquine. Singlet cells were gated (Fig. 4B)

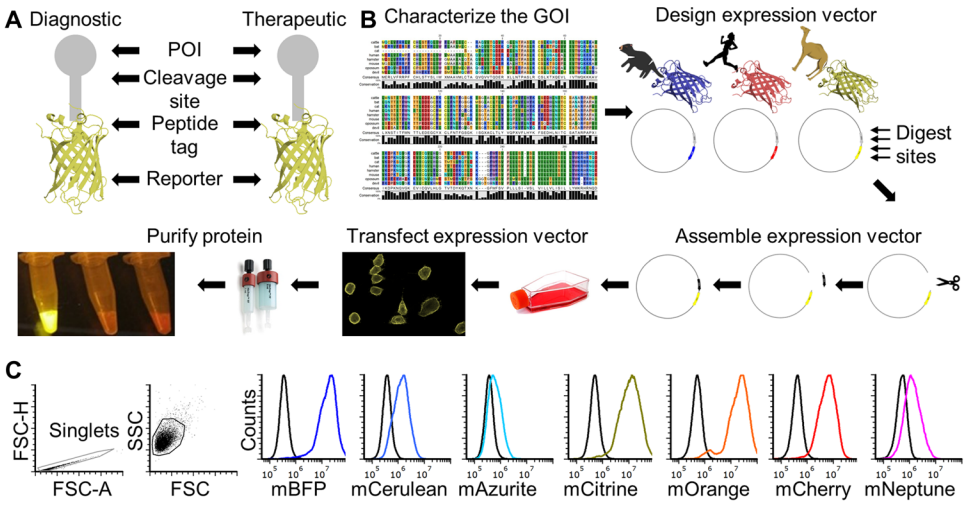

Fig. 2. FAST protein schematic and initial testing. (**A**) Schematic diagram of FAST protein therapeutic and diagnostic (i.e., theranostic) features. POI, protein of interest. (**B**) Graphic overview of FAST protein system including key steps: (i) characterize gene of interest (GOI) in silico; (ii) design expression vectors; (iii) digest FAST base vectors and insert alternative genes of interest or colors; (iv) transfect FAST vectors into mammalian cells and monitor using fluorescent microscopy or flow cytometry; (iv) purify the protein using 6xHis tag, visualize fluorescent color to show that protein is in frame and correctly folded. Image of microfuge tubes shows 100 μl of mCitrine, mOrange, and mCherry FAST proteins (1 mg/ml) excited with blue light with an amber filter. Full protocols for vector construction and protein testing are available in the Supplementary Materials. (**C**) Results of flow cytometry binding assay with devil 41BB FAST proteins. The colored lines in the histograms show binding of devil 41BB fused to mTagBFP, mCerulean3, mAzurite, mCitrine, mOrange, mCherry, or mNeptune2 to CHO cells transfected with devil 41BBL, and the black lines show binding to untransfected CHO cells. FSC, forward scatter; SSC, side scatter.

and binding of mCherry FAST proteins to carboxyfluorescein diacetate succinimidyl ester (CFSE) or mCitrine-labeled target cells was analyzed (Fig. 4C). The strongest fluorescent signal from 41BB-mCherry, 41BBL-mCherr, and CD80-Fc-mCherry was detected when cocultured with their predicted receptors, 41BBL, 41BB, and CTLA4, respectively.

Optimization of the FAST-Fc construct

The fluorescent binding signal of CD80-Fc-mCherry was lower than expected, so we next reexamined our Fc tag construct. In humans and all other mammals examined to date, the immunoglobulin G (IgG) heavy chain has glycine-lysine (Gly-Lys) residues at the C terminus; the initial devil IgG constant region sequence available to us had an incomplete C terminus, and thus, our initial CD80-Fc-mCherry vector did not have the C-terminal Gly-Lys. We subsequently made a new FAST-Fc construct with CTLA4-Fc-mCherry, which exhibited strong binding to both CD80 and CD86 transfected DFT cells (Fig. 4D).

CD200 mRNA and protein are highly expressed in DFT cells

Analysis of previously published devil and DFT cell transcriptomes suggested that CD200 mRNA is highly expressed in DFT2 cells and peripheral nerves, moderately expressed in DFT1 cells, and lower in other healthy devil tissues (Fig. 5A) (*25*, *26*, *28*). As CD200 is an inhibitory molecule expressed on most human neuroendocrine neoplasms (*29*), and both DFT1 and DFT2 originated from Schwann cells (*26*, *30*), we sought to investigate CD200 expression on DFT cells at the protein level. Staining of wild-type DFT1 and DFT2 cells with CD200R1-mOrange FAST protein showed minimal fluorescent signal (Fig. 5B). However, overexpression of CD200 using a human EF1α promoter yielded a detectable signal with CD200R1-mOrange binding to CD200 on DFT1 cells. A weak signal from CD200-mOrange was detected on DFT1 cells overexpressing CD200R1 (Fig. 5B). To confirm naturally expressed CD200 on DFT cells, we digested CD200 and 41BB FAST proteins using tobacco etch virus (TEV) protease to remove the linker and fluorescent reporter. The digested proteins were then used to immunize mice for polyclonal serum production. We stained target CHO cell lines with preimmune or immune mouse sera collected after three-times immunizations. Only the immune sera showed strong binding to the respective CD200 and 41BB target cell lines (Fig. 5C). After the final immunization (four times), we collected another batch of sera and tested it on DFT1 and DFT2 cells (Fig. 5D). In agreement with the transcriptomic data for DFT cells (*25*), the polyclonal sera revealed high levels of CD200 on DFT cells, but low levels of 41BB.

Overexpression of CD200R1 blocks surface expression of CD200

In humans, overexpression of some checkpoint proteins can block surface expression of heterophilic binding partners in cis (e.g., CD80 and PDL1) (*31*). As a potential route for disrupting the inhibitory effects of CD200 on antitumor immunity, we tested whether overexpression of CD200R1 on DFT cells could reduce CD200 surface expression. We stained a DFT1 strain, C5065, and DFT1 C5065 cells transfected to overexpress CD200 or CD200R1 with polyclonal anti-CD200 sera and secondary anti-mouse IgG Alexa Fluor 647 (AF647). We detected no surface protein expression of CD200 DFT1 cells overexpressing CD200R1 (Fig. 5E).

Identification of DFT cells in whole blood using anti-CD200

In addition to high expression of CD200 on neuroendocrine neoplasms (*29*), CD200 is used as a diagnostic marker for several human blood cancers (*32*). DFT cells metastasize in the majority of cases (*33*), and our transcriptome results (Fig. 5A) suggest that CD200 mRNA is more highly expressed in DFT cells than in peripheral blood mononuclear cells (PBMCs) (*25*, *26*). As a result, we tested whether CD200 could be used to identify DFT cells in blood. We stained PBMCs and DFT2 cells separately with polyclonal anti-CD200 sera

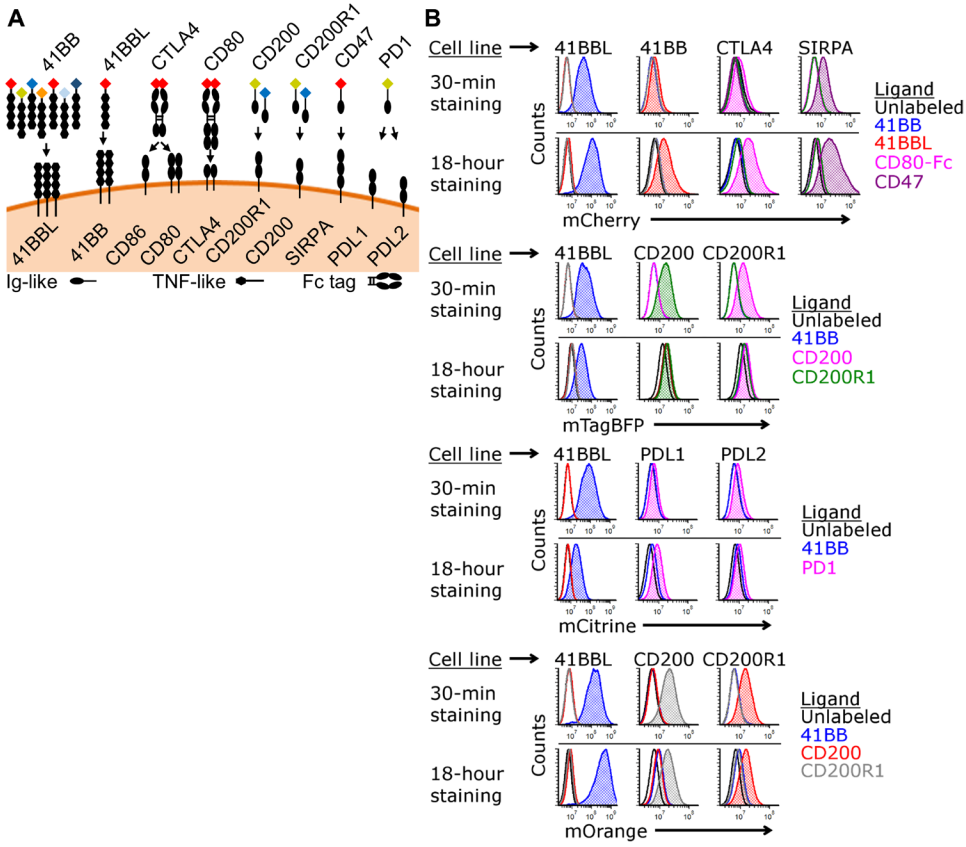

Fig. 3. Map and testing of soluble proteins FAST proteins. (**A**) Diagram of soluble FAST proteins and full-length proteins used for testing of FAST proteins. 41BBL is a type II transmembrane protein; all other proteins are type I. CD80 and CTLA4 soluble FAST proteins included a devil immunoglobulin G (IgG) Fc tag. Arrows indicate interactions confirmed in this study. TNF, tumor necrosis factor. (**B**) Histograms showing binding of FAST proteins to CHO cells expressing full-length devil proteins. Target CHO cells were cultured with chloroquine to block lysosomal degradation of FAST proteins and maintain fluorescent signal during live-culture binding assays with purified FAST proteins (2 μg per well) for 30 min or 18 hours to assess receptor-ligand binding ($N = 1$ per time point).

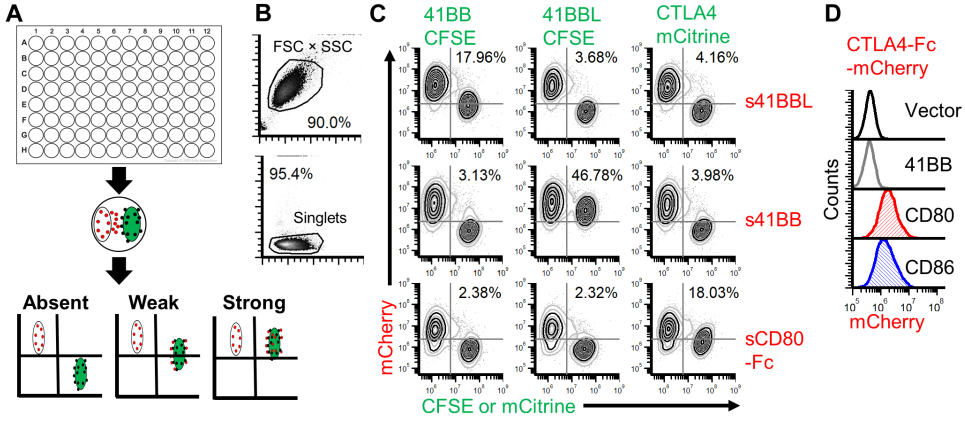

Fig. 4. Live-cell coculture assays with FAST proteins. (**A**) Schematic of coculture assays to assess checkpoint molecule interactions (absent, weak, and strong). Cells were mixed and cultured overnight with chloroquine. Protein binding and/or transfer were assessed using flow cytometry. (**B**) Gating strategy for coculture assays. (**C**) CHO cells that secrete 41BBL-mCherry, 41BB-mCherry, or CD80-Fc-mCherry were cocultured overnight with target CHO cells that express full-length 41BB, 41BBL, or CTLA4. 41BB and 41BB-L were labeled with CFSE, whereas full-length CTLA4 was directly fused to mCitrine. Cells that secrete mCherry FAST proteins appear in the upper left quadrant. Cells expressing full-length proteins and labeled with CFSE or mCitrine appear in the lower right quadrant. Cells in the upper right quadrant represent binding of mCherry FAST proteins to full-length proteins on carboxyfluorescein diacetate succinimidyl ester (CFSE) or mCitrine-labeled cells. Results shown are representative of $n = 3$ per treatment. (**D**) CTLA4-Fc-mCherry FAST protein binding to DFT cells. DFT1 C5065 cells transfected with control vector (black), 41BB (gray), CD80 (red), or CD86 (blue) were stained with CTLA4-Fc-mCherry supernatant with chloroquine. Results are representative of $N = 2$ replicates per treatment.

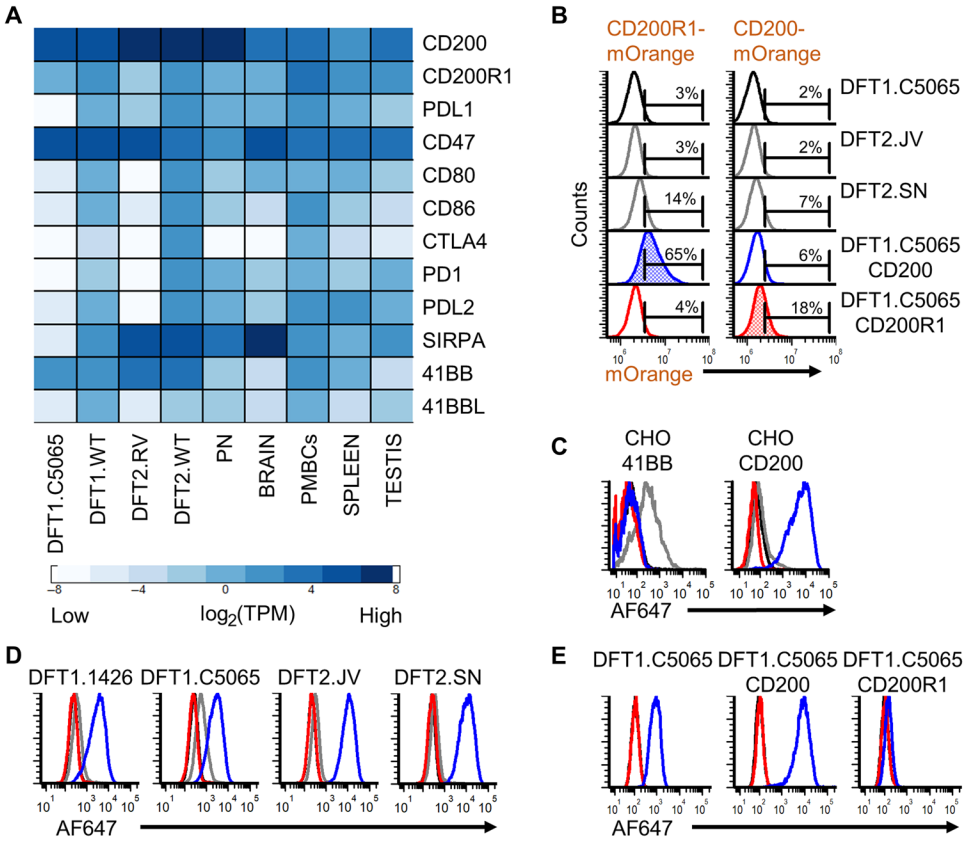

Fig. 5. Elevated CD200 expression on DFT cells. (**A**) GOIs for this study are plotted as a log_2-transformed transcripts per million (TPM) heat map with dark blue indicating the most highly expressed genes. Technical replicates ($N = 2$) from separate flasks were used for the cell lines (C5065, RV) and biological replicates ($N = 2$) were used for primary tissues, except peripheral nerve (PN) ($N = 1$). (**B**) Wild-type DFT1.C5065, DFT2.JV, DFT2.SN, and DFT1.C5065 transfected to overexpress CD200 or CD200R1 were stained with either CD200R1-mOrange or CD200-mOrange FAST protein. Histograms filled with blue or red highlight expected strong binding interactions. The percentage of events that falls within the marker is shown. Results are representative of $N = 2$ replicates per treatment. (**C**) Mice were immunized with 41BB or CD200 FAST proteins. Black, preimmune; gray, immune sera from a mouse immunized with 41BB; red, preimmune; blue, immune sera from a mouse immunized with CD200. CHO cells transfected with either full-length 41BB or CD200 were stained with sera and then anti-mouse AF647. Results are representative of $N = 2$ per treatment. (**D**) Sera were used to screen two strains each of DFT1 and DFT2 cells for 41BB and CD200 expression. Results are representative of $N = 3$ per treatment. (**E**) DFT1 C5065 transfected with either vector control, CD200, or CD200R1 was stained with purified polyclonal anti-CD200 and anti-mouse IgG AF647 (black, no antibodies; red, secondary antibody only; blue, primary and secondary antibody). Results are representative of $N = 2$ per treatment.

and anti-mouse AF647 and then analyzed CD200 expression by flow cytometry (fig. S4A). We then mixed the stained PBMCs and DFT2 cells at ratios of 1:10 (fig. S4A) and 1:5 (fig. S4B) and analyzed the mixed populations. PBMCs showed minimal CD200 expression and background staining (fig. S4), whereas CD200 was highly expressed on DFT2 cells. $CD200^+$ DFT2 cells were readily distinguishable from PBMCs.

As our RNA sequencing (RNA-seq) results only included mononuclear cells, we next performed a pilot test to determine whether DFT cells could be spiked into whole devil blood and identified via flow cytometry using CD200 staining. DFT1 and DFT2 cells were labeled with CellTrace violet (CTV), and 10,000 cells were diluted directly into 100 µl of whole blood from a healthy devil ($N = 1$ per treatment; $n = 1$ devil). The cells were then stained with purified polyclonal anti-CD200 with and without secondary anti-mouse IgG AF647 before red blood cell (RBC) lysis. Initial results showed that DFT2 cells expressed CD200 above the leukocyte background but that DFT1 cells could not be distinguished from leukocytes (fig. S5). To eliminate the secondary antibody step from the whole blood staining protocol, we next labeled the polyclonal anti-CD200 and normal mouse serum (NMS) with a no-wash Zenon mouse IgG AF647 labeling reagent ($n = 1$ per treatment; $n = 2$ devils). This system again showed that CD200 expression could be used to identify DFT2 cells in blood (Fig. 6, A to E), suggesting that CD200 is a candidate marker for identification of metastasizing DFT2 cells.

FAST nanobody proof of concept

Last, to test whether the FAST system could be applied to other species (e.g., camelid-derived nanobody) and applications (FAST nanobody), we reverse-translated the protein sequence for an anti-human PDL1 nanobody (*24*) and inserted the codon-optimized DNA sequence into a FAST mCitrine vector. The assembled plasmid was transfected into ExpiCHO cells, and the supernatant was tested for binding to CHO cells stably transfected with either full-length human PDL1 or human CD80; the human proteins were fused to miRFP670 (Addgene no. 79987) in a FAST vector. The nanobody supernatant was used undiluted or at 1:10 or 1:100 dilutions. The nanobody showed strong binding to PDL1-expressing cells, but not CD80-expressing cells (Fig. 6F).

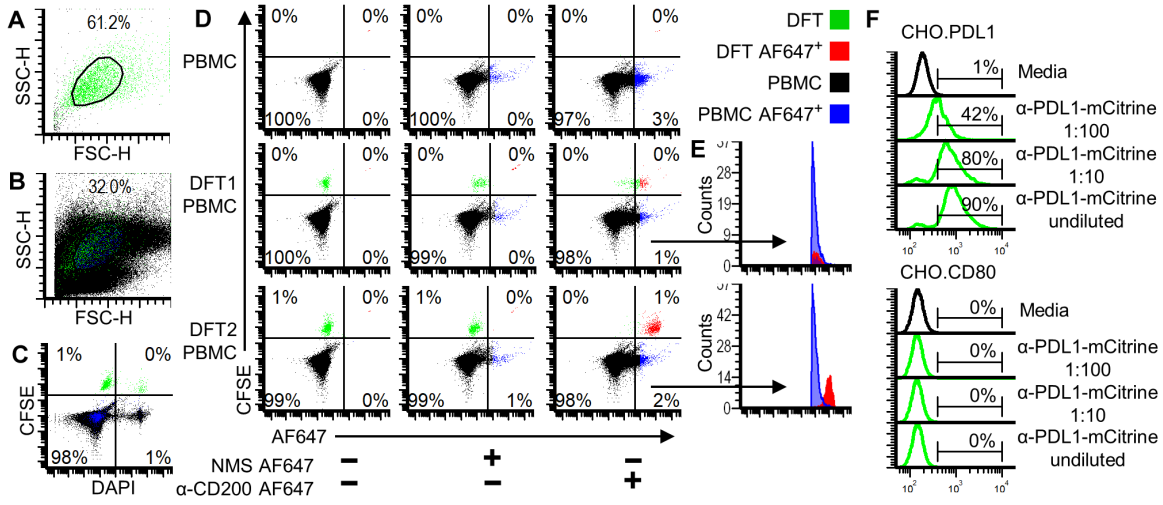

Fig. 6. CD200 identifies DFT cells in whole blood and nanobody testing. Color dot plots showing DFT cells in green (CFSE), PBMCs in black, DFT Alexa Fluor 647$^+$ (AF647$^+$) cells in red, and PBMC AF647$^+$ in blue. Forward- and side-scatter plot of DFT2.JV cells alone (**A**) and DFT2.JV cells mixed with PBMCs (**B**). (**C**) Color dot plot showing dead cells stained with 4′,6-diamidino-2-phenylindole (DAPI) (right quadrants) and CFSE-labeled DFT cells (upper quadrants). (**D**) The top row shows unmixed PBMCs. The middle row and bottom row show PBMCs mixed with DFT1.C5065 (middle) and DFT2.JV (bottom) cells. Cell mixtures were either untreated or incubated with Zenon AF647–labeled NMS or Zenon AF647–labeled α-CD200 serum. AF647$^+$ DFT (red) and PBMC (blue) are in the right quadrants. (**E**) Histogram overlays to highlight AF647$^+$ (right quadrants) from DFT1-PBMC and DFT2-PBMC mixtures. Cells were analyzed on the Beckman Coulter MoFlo Astrios. (**F**) FAST nanobody proof of concept was accomplished using supernatant from untransfected ExpiCHO cells or ExpiCHO cells secreting human anti–PDL1-mCitrine nanobody. Nanobody supernatant was used undiluted or at 1:10 or 1:100 dilutions in media and used to stain CHO cells that express either human PDL1 or human CD80. Results are representative of $N = 2$ per treatment.

DISCUSSION

Naturally occurring cancers provide a unique opportunity to study immune evasion and the metastatic process across diverse hosts and environments. The exceptionally high cancer rate in Tasmanian devils coupled with the two transmissible tumors currently circulating in the wild warrants a thorough investigation of the devil immune system. However, taking advantage of these natural disease models has been out of reach for most species because of a lack of reagents. The FAST protein system that we developed here is well suited to discovering additional DFT markers and, more generally, to filling the reagent gap for nontraditional species. For proteins like 41BB that have high affinity for 41BBL, FAST proteins can be used as detection reagents directly from supernatant. For other molecules with lower receptor-ligand affinity, the FAST proteins can be purified, digested with a protease to remove the nontarget proteins, and used for production of higher-affinity binding proteins (e.g., antibodies, aptamers, and nanobodies).

The versatility of the FAST system was demonstrated by fusing a validated human anti-PDL1 nanobody derived from a camel (*Camelus bactrianus*) heavy-chain variable region to mCitrine. The nanobody-reporter fusion allowed direct testing of the nanobody from supernatant without the need for purification or secondary labeling and provided a 1:1 ratio of nanobody and reporter to allow quantification of target proteins. In addition to fusing nanobodies to fluorescent proteins, fluorescently labeled target proteins could be used with nanobody display libraries to pull down or sort nanobodies that bind the target protein.

The simple cut-and-paste methods for vector assembly lend the FAST protein system to entry-level immunology and molecular biology skill sets. In addition, the ability of FAST proteins to be used in live coculture assays and with elimination of secondary reagents will increase efficiency and reduce experimental error for advanced human and mouse cancer immunology studies. For example, previous high-throughput studies have used a two-step staining process (i.e., recombinant protein and secondary antibody) to screen more than 2000 protein interactions (*34*); this type of assay can be streamlined using FAST proteins to eliminate the need for secondary antibodies. Fc tags or other homodimerization domains can be incorporated into FAST proteins to increase binding for low-affinity interactions and to assess potential Fc receptor–mediated functions.

Production of recombinant proteins in cell lines that closely resemble the physiological conditions of the native cell type (i.e., mammalian proteins produced in mammalian cell lines) is more likely to yield correct protein folding, glycosylation, and function than proteins produced using evolutionarily distant cell lines. The fluorescent fusion proteins developed here take advantage of natural receptor expression and cycling processes (e.g., CTLA4 transendocytosis) in eukaryotic target cells; bacterial protein production methods are not amenable to coculture with eukaryotic target cells in immunological assays. Our demonstration of the FAST protein system in CHO cells suggest that this method can be efficiently integrated into existing research and development pipelines for humans and other vertebrate species.

A primary question in transmissible tumor research is why genetically mismatched cells are not rejected by the host. Successful infection of devils with DFT cells relies on the ability of the tumor allograft to evade and manipulate host defenses. The "missing-self" hypothesis suggests that the lack of constitutive MHC-I expression on DFT1 cells should lead to natural killer (NK) cell–mediated killing of the allograft tumor cells. Here, we used the FAST protein system to develop a tool set to address this question and show that DFT1 and DFT2 cells express CD200 at higher levels than most other devil tissues examined to date. CD200 has been shown to directly inhibit NK cells in other species (*35*), so overexpression of CD200 is a potential mechanism of immune evasion of NK responses by DFT cells.

We hypothesize that CD200 could be particularly important in DFT transmission as the CD200-CD200R pathway is critical to the initial stages of establishing transplant and allograft tolerance in other species (*36*). In line with this hypothesis, a recent study reported that overexpressing several checkpoint molecules, including CD200, PDL1, and CD47, in mouse embryonic stem cells could be used to generate teratomas that could establish long-term allograft tolerance in fully immunocompetent hosts (*37*). We have previously reported that PDL1 mRNA and protein are up-regulated on DFT2 cells in response to IFN-γ (*17*), and our transcriptome results show that CD47 is expressed at moderate to high levels in DFT cells. Here, we show that overexpression of CD200R1 on DFT1 eliminates binding of our polyclonal anti-CD200 antibodies, suggesting that DFT cells overexpressing CD200R1 could be used to test the role of CD200 in allograft tolerance. Alternatively, genetic ablation of CD200 in DFT cells could be used as a complementary approach to examine the role of immune checkpoint molecules in DFT allograft tolerance. Low MHC-I expression is a primary means of immune evasion by DFT1 cells, and disrupting the CD200-CD200R1 pathway could facilitate improved recognition of DFT1 cells by CD8 T cells by enhancing IFN-γ–mediated MHC-I up-regulation. Recent work in mice has identified immunosuppressive natural regulatory plasma cells that express CD200, LAG3, PDL1, and PDL2; we have previously identified $PDL1^+$ cells with plasma cell morphology near or within the DFT microenvironment (*17*).

Previous DFT vaccine efforts have used killed DFT cells with adjuvants (*38*, *39*). A similar approach to treat gliomas in dogs reported that tumor lysate with CD200 peptides nearly doubled progression-free survival compared to tumor lysate alone (*40*). Like devils, several breeds of dog are prone to cancer, and these genetically outbred large animal models provide a fertile ground for testing cancer therapies. The CD200 peptides are reported to provide agonistic function through CD200-like activation receptors (CD200R4) rather than by blocking CD200R1 (*40*). The functional role of CD200-CD200R pathway in devils remains to be elucidated, but the $CD200R1_{NPLY}$ inhibitory motif and key tyrosine residues are conserved in devil CD200R (*19*, *41*, *42*), demonstrating that this motif is conserved over 160 million years of evolutionary history (*43*). In addition to agonistic peptides, several other options for countering CD200-CD200R immune inhibition are possible. Human chronic lymphocytic leukemia cells often express high levels of CD200, which can be down-regulated in response to imiquimod (*44*). Likewise, we have previously shown that DFT1 cells down-regulate expression of CD200 mRNA in vitro in response to imiquimod treatment (*25*). In one of the longest running and most in-depth studies of host-pathogen coevolution, CD200R was shown to be under selection in rabbits in response to a myxoma virus biocontrol agent (*45*). As DFT1 and DFT2 have been circulating in devils for more than 20 and 5 years, respectively, it will be important to monitor CD200/R expression and the potential evolution of paired activating and inhibitory receptors in these natural disease models.

Immunophenotyping and single-cell RNA-seq of CTCs have a potential to identify key gene expression patterns associated with metastasis and tissue invasion. CD200 is a potential marker for the identification of CTCs from devil blood. As proof of concept, DFT2 cells could be identified in devil blood spiked with DFT2 cells. As CTCs are likely to be rare in the blood of most infected devils, CD200 alone would be insufficient for identifying DFT1 cells. Additional surface DFT markers would be required to purify CTCs for metastases and tissue invasion analyses. The FAST protein system provides a simple procedure to facilitate the production of a panel of DFT markers to help identify key proteins in the metastatic process.

In summary, the simple "cut-and-paste" production of the vectors and single-step testing pipeline of the FAST system provided multiple benefits. The FAST system allowed us to characterize receptor-ligand interactions and to identify evolutionarily conserved immune evasion pathways in naturally occurring transmissible cancers. Our initial implementation of the system confirmed numerous predicted protein interactions in a marsupial species and documented high expression of the inhibitory molecule CD200 on DFT cells. The high expression of CD200 in devil nervous tissues and neuroendocrine tumors, down-regulation of CD200 in response to imiquimod, and binding of CD200 to CD200R1 are consistent with results from human and mouse studies. Consequently, the CD200/R pathway provides a promising immunotherapy and vaccine target for DFTs (*20*). Beyond this study, FAST proteins meet the key attributes needed for reagent development, such as being straightforward to make, stable, versatile, renewable, cheap, and amenable to high-throughput testing. The direct fusion of the reporter protein to the protein of interest allows for immediate feedback during transfection, supernatant testing, and protein purification; proteins with frameshifts, introduced stop codons, or folded improperly will not fluoresce and can be discarded after a simple visualization, rather than only after extensive downstream testing. Efficient mapping of immune checkpoint interactions across species can identify evolutionarily conserved immune evasion pathways and appropriate large-animal models with naturally occurring cancer. This knowledge could inform veterinary and human medicine in the fields of immunological tolerance to tissue transplants, infectious disease, and cancer.

MATERIALS AND METHODS

Experimental design

The objectives of this study were to fill a major gap in our understanding of the mammalian immune system and to understand how genetically mismatched transmissible tumors evade host immunity. To achieve this goal, we developed a recombinant protein system that directly fuses proteins of interest to a fluorescent reporter protein. The first phase was to determine whether the fluorescent protein remained fluorescent after secretion from mammalian cells and to confirm that proteins bound to their predicted receptors (i.e., ligands). Initial testing was performed in CHO cells and follow-up assays used devil cells. To reduce the risk of false positives in binding assays, we tested each FAST protein against the expected target protein and additional nontarget proteins. To further demonstrate the functionality of this system for antibody development, mice were immunized with either 41BB or CD200 proteins. Pre- and postimmunization polyclonal sera were used to confirm that the proteins used for immunization induced antibodies that specifically bound to surface-expressed recombinant proteins and native proteins on DFT cells. Last, to demonstrate the flexibility of the system, we replicated a known anti-human PDL1 nanobody that we fused to mCitrine. This shows that the FAST system can be used to target human proteins, to produce recombinant proteins derived from other species (e.g., camelid-derived nanobody), and for functions other than receptor-ligand interactions.

Target transcript amplification

Target gene DNA sequences for vector construction were retrieved from Genbank, Ensembl, or de novo transcriptome assemblies

(table S2). Target DNA was amplified from a complementary DNA template or existing plasmids using primers and polymerase chain reaction (PCR) conditions shown in tables S2 and S4 using Q5 High-Fidelity 2X Master Mix (New England Biolabs no. M0494L). Primers were ordered with 5′ base extensions that overlapped expression vectors on either side of the restriction sites. The amplified products were identified by gel electrophoresis and purified using the NucleoSpin PCR and Gel Clean Up Kit (Macherey-Nagel no. 740609.5). Alternatively, DNA sequences were purchased as double-stranded DNA gBlocks (table S5) (Integrated DNA Technologies) for direct assembly into expression vectors.

Construction of all-in-one Sleeping Beauty transposon vectors

All new plasmids were assembled using the NEBuilder kit (New England Biolabs; NEB no. E5520S) following the manufacturer's recommendations unless otherwise noted. DNA inserts, digested plasmids, and NEBuilder master mix were incubated for 60 min at 50°C and then transformed into DH5α included with the NEBuilder kit. Plasmid digestions were performed following manufacturer recommendations and generally subjected to Antarctic phosphatase (New England Biolabs no. M0289S) treatment to prevent potential reannealing. Sleeping Beauty transposon vectors pSBbi-Hyg (Addgene no. 60524), pSBbi-BH (Addgene no. 60515), pSBtet-Hyg (Addgene no. 60508), and pSBtet-RH (Addgene no. 60500) were gifts to Addgene from E. Kowarz (*46*). The pCMV (CAT)T7-SB100 containing the cytomegalovirus (CMV) promoter and SB100X transposase was a gift to Addgene from Z. Izsvak (Addgene no. 34879) (*47*). We first constructed an all-in-one Sleeping Beauty vector by inserting a CMV promoter and SB100X transposase from pCMV(CAT)T7-SB100 (*47*) into pSBi-BH (*46*) (tables S3 and S4). This was accomplished by using pAF111-vec.FOR and pAF111.1.REV primers to amplify an overlap region from pSBbi-BH (insert 1) and pAF111-2.FOR and pAF111-2.REV to amplify the CMV-SB100X region from pCMV(CAT)T7-SB100 (insert 2). The purified amplicons were then used for NEBuilder assembly of pAF111. The final all-in-one vectors pAF112 (hygromycin resistance and luciferase) and pAF123 (hygromycin resistance) were assembled from the pAF111 components. pAF112 was assembled by amplifying the Luc2 luciferase gene (insert 1) from pSBtet-Hyg and the P2A-hygromycin resistance gene (insert 2) from pSBbi-BH and inserting into the pAF111 Bsu36 I digest using NEBuilder. pSBbi-Hyg was Bsu36 I–digested to obtain the hygromycin resistance gene, and this fragment was inserted into Bsu36 I–digested pAF111 using T4 ligase cloning to replace the BFP-P2A-hygromycin segment in pAF111.

Construction of full-length protein vectors

All full-length gene coding sequences except CTLA4 were cloned into the pAF112 Sfi I digest (table S2). All full-length vectors also contain luciferase with T2A peptide linked to the hygromycin resistance protein; luciferase was included for use in downstream functional testing that was not part of this study. Tasmanian devil CTLA4 was cloned into a NotI-HF and Xma I digest of pAF100 that was used in a different study but is derived from vectors pAF112 and pAF138. In addition, we also used devil PDL1 (CHO.pAF48) and 41BBL (CHO.pAF56) cell lines developed using a vector system described previously (*17*).

Construction of FAST protein vectors

Plasmids containing fluorescent protein coding sequences mCerulean3-N1 (Addgene no. 54730), mAzurite-N1 (Addgene no. 54617), mOrange-N1 (Addgene no. 54499), and mNeptune2-N1 (Addgene no. 54837) were gifts to Addgene from M. Davidson. mTag-BFP was amplified from pSBbi-BH, mCitrine was amplified from pAF71, and mCherry was amplified from pTRE-Dual2 (Clontech no. PT5038-5). pAF137 was constructed by amplifying the devil 41BB extracellular domain with primers pAF137-1.FOR and pAF137-1.REV and amplifying mCherry with pAF137-2a.FOR and pAF137-2.REV (tables S3 and S4). 5′ extensions on pAF137-1.FOR and pAF137-2.REV were used to create overlaps for NEBuilder assembly of pAF137 from a pAF123 Sfi I–digested base vector. 3′ extensions on pAF137-1.REV and pAF137-2a.FOR were used to create the linker that included an Xma I/Sma I restriction site, TEV cleavage tag, GSAGSAAGSGEF linker peptide, and 6xHis tag between the gene of interest and fluorescent reporter. The GSAGSAAGSGEF was chosen because of the low number of large hydrophobic residues and less repeated nucleic acids than are needed with other flexible linkers such as $(GGGS)_4$. The pAF137 primer extensions also created 5′ Not I and 3′ Nhe I sites in the FAST vector to facilitate downstream swapping of functional genes and to create a Kozak sequence (GCCGCCACC) upstream of the FAST protein open-reading frame. Following confirmation of correct assembly via DNA sequencing, the FAST 41BB-mCherry (pAF137) was digested and used as the base vector (Fig. 2B and fig. S1, A and B) for development of FAST vectors with alternative fluorescent proteins. This was accomplished by digestion of pAF137 with Sal I and Nhe I and then inserting PCR-amplified coding sequences for other fluorescent proteins using NEBuilder (tables S3 and S4).

Type I FAST (extracellular N terminus and cytoplasmic C terminus) protein vectors were constructed by digestion of 41BB FAST vectors with Not I and either Xma I or Sma I (Fig. 2B and fig. S1, A and B) and then inserting genes of interest (tables S2 to S4). To create an Fc-tagged FAST protein, we fused the extracellular domain of devil CD80 to the Fc region of the devil IgG (fig. S1C). The Fc region was amplified from a devil IgG plasmid provided by L. Corcoran (Walter and Eliza Hall Institute of Medical Research). All secreted FAST proteins in this study used their native signal peptides, except for 41BBL. 41BBL is a type II transmembrane protein in which the signal peptide directly precedes the cytoplasmic and transmembrane domains of the protein (cytoplasmic N terminus and extracellular C terminus). As type I FAST vectors cannot accommodate this domain architecture, we developed an alternative base vector for type II transmembrane FAST proteins (fig. S1D). To increase the probability of efficient secretion of type II FAST proteins from CHO cells, we used the hamster interleukin-2 (IL-2) signal peptide (accession no. NM_001281629.1) at the N terminus of the protein, followed by a Sal I restriction site, mCherry, an Nhe I restriction site, 6xHis tag, GSAGSAAGSGEF linker, TEV cleavage site, Xma I/Sma I restriction site, the gene of interest, and a Pme I restriction site following the stop codon.

General plasmid assembly, transformation, and sequencing

Following transformation of assembled plasmids, colony PCR was performed as an initial test of the candidate plasmids. Single colonies were inoculated directly into a OneTaq Hot Start Quick-Load 2X Master Mix (NEB no. M0488) with primers pSB_EF1a_seq.FOR (atcttggttcattctcaagcctcag) and pSB_bGH_seq.REV (aggcacagtcgaggctgat). PCR was performed with 60°C annealing temperature for 25 to 35 cycles. Colonies yielding appropriate band sizes were used to inoculate Luria broth with ampicillin (100 μg/ml) for bacterial outgrowth overnight at 37°C and 200 rpm. The plasmids were purified using standard plasmid kits and prepared for Sanger sequencing using

the BigDye Terminator v3.1 Cycle Sequencing Kit (Thermo Fisher Scientific no. 4337455) with pSB_EF1a_seq.FOR and pSB_bGH_seq.REV primers. The BigDye Terminator was removed using Agencourt CleanSEQ (Beckman Coulter no. A29151) before loading samples to a 3500xL Genetic Analyzer (Applied Biosystems) for sequencing by fluorescence-based capillary electrophoresis.

General cell culture conditions

DFT1 cell line C5065 and DFT2 cell line JV were cultured at 35°C with 5% CO_2 in cRF10 [10% complete RPMI (Gibco no. 11875-093) with 2 mM L-glutamine, supplemented with 10% heat-inactivated fetal bovine serum, and 1% antibiotic-antimycotic (Thermo Fisher Scientific no. 15240062)]. RPMI without phenol red (Sigma-Aldrich no. R7509) was used to culture FAST protein cell lines when supernatants were collected for downstream flow cytometry assays. Devil peripheral blood cells were cultured in cRF10 at 35°C with 5% CO_2. CHO cells were cultured at 37°C in cRF10 during transfections and drug selection but were otherwise cultured at 35°C in cRF5 (5% complete RPMI). For production of purified recombinant proteins, stably transfected CHO cells were cultured in suspension in spinner flasks in chemically defined, serum-free CHO EX-CELL (Sigma-Aldrich no. 14361C) media supplemented with 8 mM L-glutamine, 10 mM Hepes, 50 μM 2-ME, 1% (v/v) antibiotic-antimycotic, and 1 mM sodium pyruvate and without hygromycin.

Transfection and generation of recombinant cell lines

Stable transfections of CHO and DFT cells were accomplished by adding 3×10^5 cells to each well in six-well plates in cRF10 and allowing the cells to adhere overnight. The next day, 2 μg of plasmid DNA was added to 100 μl of phosphate-buffered saline (PBS) in microfuge tubes. Polyethylenimine (PEI) (linear, molecular weight, 25,000; Polysciences no. 23966-2) was diluted to 60 μg/ml in PBS and incubated for at least 2 min. The PEI solution (100 μl) was added to the 100 μl of plasmid DNA in each tube to achieve a 3:1 ratio of PEI:DNA. The solution was mixed by gentle pipetting and incubated at room temperature for 15 min. While the solution was incubating, the media on the CHO cells were replaced with fresh cRF10. All 200 μl from each DNA:PEI mix was then added dropwise to the CHO cells and gently rocked side to side and front to back to evenly spread the solution throughout the well. The plates were then incubated overnight at 37°C with 5% CO_2. The next day, the plates were inspected for fluorescence, and then the media were removed and replaced with cRF10 containing hygromycin (1 mg/ml) (Sigma-Aldrich no. H0654). The media were replaced with fresh cRF10 hygromycin (1 mg/ml) every 2 to 3 days for the next 7 days until selection was complete. The cells were then maintained in hygromycin (0.2 mg/ml) in cRF5 at 35°C with 5% CO_2. Supernatant was collected 2 to 3 weeks after transfection and stored at 4°C for 2 months to assess stability of secreted FAST proteins.

Protein production and purification

Sixteen days after transfection, the first batch of FAST protein cell lines was adapted to a 1:1 mix of cRF5 and chemically defined, serum-free CHO EX-CELL media for 1 to 2 days to facilitate adaptation of the adherent CHO cells to suspension culture in serum-free media. At least 5×10^7 cells were then transferred to ProCulture spinner flasks (Sigma-Aldrich no. CLS45001L and no. CLS4500250) and stirred at 75 rpm at 35°C in 5% CO_2 on magnetic stirring platforms (Integra Bioscience no. 183001). Cells were maintained at a density ranging from 5×10^5 to 2×10^6 cells/ml for 8 to 14 days. Supernatant was collected every 2 to 3 days, centrifuged at 3200 relative centrifugal force (RCF) for 10 min, stored at 4°C, and then purified using the ÄKTA start protein purification system (GE Life Sciences no. 29022094). The supernatant was diluted 1:1 with 20 mM sodium phosphate (pH 7.4) and then purified using HisTrap Excel columns (GE Life Sciences no. 17-3712-05) according to the manufacturer's instructions. Samples were passed through the columns using a flow rate of 2 ml/min at 4°C; all wash and elution steps were done at 1 ml/min. Elution from HisTrap columns (GE Life Sciences no. 17-3712-05) was accomplished using 0.5 M imidazole and fractionated into 1-ml aliquots using the Frac30 fraction collector (GE Life Sciences no. 29023051). Fluorescence of FAST proteins was checked via brief excitation (Fig. 2) on a blue light transilluminator with an amber filter unit. In the case of mCherry, chromogenic color was visible without excitation. Fractions containing target proteins were combined and diluted to 15 ml with cold PBS, dialyzed (Sigma-Aldrich no. PURX60005) in PBS at 4°C, 0.22-μm sterile-filtered (Millipore no. SLGV033RS), and concentrated using Amicon Ultra centrifugal filter units (Sigma-Aldrich no. Z706345). The protein concentration was quantified using the 280-nm absorbance on a NanoDrop spectrophotometer. Extinction coefficients using for each protein were calculated using the ProtParam algorithm (*48*). The proteins were then aliquoted into microfuge tubes and frozen at −80°C until further use. The CTLA4-Fc-mCherry protein was designed, assembled, and tested separately from the other FAST proteins and was tested directly in supernatant without purification.

Preparation of CHO cells expressing full-length proteins for flow cytometry

CHO cells expressing full-length proteins were thawed in cRF10 and then maintained in cRF5 with hygromycin (0.2 mg/ml). The adherent CHO cells were washed with PBS and incubated with trypsin for 5 min at 37°C to remove cells from the culture flask. Trypsin was diluted five times with cRF5 and centrifuged at 200 RCF for 5 min. Cells were resuspended in cRF5, counted (viability >95% in all cases), and resuspended and aliquoted for assays as described below.

Initial staining of CHO cells with 41BB FAST protein supernatants (without chloroquine)

Supernatants (cRF5) were collected from CHO cells expressing devil 41BB extracellular domain fused to either mCherry (pAF137), mCitrine (pAF138), mOrange (pAF164), mBFP (pAF139), mAzurite (pAF160), mCerulean3 (pAF161), or mNeptune2 (pAF163) (tables S2 to S4). The supernatant was spun for 10 min at 3200 RCF to remove cells and cellular debris and then stored at 4°C until further use. CHO cells expressing devil 41BBL (CHO.pAF56) and untransfected CHO cells were prepared as described above. Flow cytometry tubes were loaded with 5×10^4 target CHO cells per well in cRF5, centrifuged 500 RCF for 3 min, and then resuspended in 200 μl of supernatant from the 41BB FAST cell lines ($N = 1$ per treatment). The tubes were then incubated for 15 min at 4°C, centrifuged at 500 RCF for 3 min, resuspended in 400 μl of cold fluorescence-activated cell sorting (FACS) buffer, and stored on ice until the data were acquired on a Beckman Coulter Astrios flow cytometer (Fig. 2C). All flow cytometry data were analyzed using FCS Express 6 Flow Cytometry Software version 6 (De Novo Software).

Staining CHO cells with FAST protein supernatants (without chloroquine)

U-bottom 96-well plates were loaded with 1×10^5 target CHO cells per well in cRF5, centrifuged 500 RCF for 3 min, and then resuspended

in 175 μl of cRF5 supernatant from FAST cell lines collected 11 days after transfection ($N = 1$ per treatment). The plates were then incubated for 30 min at room temperature, centrifuged at 500 RCF for 3 min, resuspended in 200 μl of cold FACS buffer, centrifuged again, and fixed with FACS fix buffer [PBS, 0.02% NaN_3, 0.4% formalin, glucose (10 g/liter)]. The cells were transferred to tubes, diluted with FACS buffer, and analyzed on a Beckman Coulter Astrios flow cytometer (fig. S2).

Staining CHO cells with purified FAST proteins (with chloroquine)

Purified FAST proteins were diluted to 20 μg/ml in cRF5, aliquoted into V-bottom 96-well transfer plates, and then stored at 37°C until target cells were ready for staining. Target cells were resuspended in cRF5 with 100 μM chloroquine, and 100,000 cells per well were aliquoted into U-bottom 96-well plates. One hundred microliters of the diluted FAST proteins ($N = 1$ per treatment, two time points per treatment) was then transferred from the V-bottom plates into the U-bottom 96-well plates containing target cells. The final volumes and concentrations were 200 μl per well in cRF5 with 50 μM chloroquine and 2 μg per well of FAST proteins. One set of plates was incubated at 37°C for 30 min, and another set of plates was incubated at 37°C overnight. The cells were then centrifuged 500 RCF for 3 min, the media decanted, and incubated for 5 min with 100 μl of trypsin to dislodge adherent cells. The cells were then washed with 200 μl of cold FACS buffer, fixed, resuspended in cold FACS buffer, and transferred to tubes for analysis on the Astrios flow cytometer (Fig. 3B).

Staining CHO cells with FAST supernatants (with chloroquine)

The protocol for using FAST protein supernatants was the same above as the preceding experiment except for the modifications described here. Supernatants were collected 2 to 3 weeks after transfection, centrifuged at 3200 RCF for 10 min, and stored at 4°C for 2 months. Before staining for flow cytometry, the supernatant was 0.22-μm filtered. Supernatant was then loaded into V-bottom 96-well plates to facilitate rapid transfer to staining plates and stored at 37°C until target cells were ready for staining. Target cells were prepared as described above except for being diluted in cRF5 with 100 μM chloroquine. A total of 2×10^5 cells per well (100 μl) were then loaded into U-bottom 96-well plates. One hundred microliters of FAST protein supernatant ($N = 1$ per treatment) was then transferred from the V-bottom plates to achieve 50 μM chloroquine, and the cells were then incubated at 37°C for 60 min. The plates were then washed, fixed, and analyzed on the Astrios flow cytometer (fig. S3). A similar procedure was used for staining stably transfected DFT cells with CTLA4-Fc-mCherry, except that the supernatant was used fresh (Fig. 4D).

Coculture assay with full-length target and FAST protein CHO cell lines (with chloroquine)

CHO cells expressing full-length CTLA4 with a C-terminal mCitrine and CHO cells expressing full-length 41BB or 41BBL were labeled with 5 μM CFSE; CFSE and mCitrine were analyzed using the same excitation laser (488 nm) and emission filters (513/26 nm). A total of 1×10^5 FAST protein–secreting cells were mixed with 1×10^5 target cells in cRF5 with 50 μM chloroquine and incubated overnight at 37°C in 96-well U-bottom plates (Fig. 4A). The next day, the cells were rinsed with PBS, trypsinized, washed, fixed, and resuspended in FACS buffer before running flow cytometry. Cells were gated on forward and side scatter (FSC × SSC) and for singlets (FSC-H × FSC-A) (Fig. 4B). Data shown in Fig. 4C are representative of $N = 3$ technical replicates per treatment. Data were collected using a Beckman Coulter MoFlo Astrios and analyzed using FCS Express.

Analysis of checkpoint molecule expression in DFT cells and Tasmanian devil tissues

RNA-seq data were generated during previous experiments, aligned against the reference Tasmanian devil genome Devil_ref v7.0 (GCA_000189315.1), and summarized into normalized read counts as previously described (*25*, *26*). Transcripts per million–normalized read counts were calculated in R, and a heat map was produced from $\log_2$-converted values using the heatmap.2 function of gplots.

Staining DFTs cell with CD200/R FAST proteins

A total of 50,000 DFT cells per well were aliquoted into U-bottom 96-well plates, washed with 150 μl of cRF10, and resuspended in 100 μl of warm cRF10 containing 100 μM chloroquine. Five micrograms of FAST protein per well was then added and mixed by pipetting. The plates were then incubated at 37°C for 30 min. The cells were then transferred to microfuge tubes without washing, stored on ice, and analyzed on a Beckman Coulter MoFlo Astrios ($N = 2$ per treatment).

Polyclonal antibody development

CD200 and 41BB FAST proteins were digested overnight with TEV protease (Sigma-Aldrich no. T4455) at 4°C in PBS. The cleaved linker and 6xHis tag were then removed using a His SpinTrap kit (GE Healthcare no. 28-9321-71). Digested proteins in PBS were diluted 1:1 in Squalvax (OZ Biosciences no. SQ0010) to a final concentration of 0.1 μg/μl and were mixed using interlocked syringes to form an emulsion. Immunization of BALB/c mice for antibody production was approved by the University of Tasmania Animal Ethics Committee (no. A0014680). Preimmune sera were collected before subcutaneous immunization with at least 50 μl of the emulsion. On day 14 after immunization, the mice were boosted using a similar procedure. On day 50, the mice received a booster with proteins in IFAVax (OZ Biosciences no. IFA0050); mice immunized with CD200 again received subcutaneous injections, whereas 41BB mice received subcutaneous and intraperitoneal injections. Preimmune and sera collected after three-times immunizations were then tested by flow cytometry against CHO cells expressing either 41BB or CD200. CHO cells were prepared as described above, and 2×10^5 cells were incubated with mouse serum diluted 1:200 in PBS for 30 min at 4°C. The cells were then washed two times and stained with 50 μl of anti-mouse IgG AF647 diluted 1:1000 in FACS buffer. The cells were then washed two times, stained with 4′,6-diamidino-2-phenylindole (DAPI) to identify live cells, and analyzed on a CyAn ADP flow cytometer (Fig. 5C). CD200 and 41BB expression on DFT cells was tested using a procedure similar to the CHO cell staining, except that the sera used were collected after four-times immunizations and was diluted 1:500 and analyzed on the BD FACSCanto II (Fig. 5D).

Purification of antibodies from NMS and anti-CD200 serum

Approximately, 200 μl of NMS or anti-CD200 serum day 157 (after four-times immunizations) was purified using an Ab SpinTrap (GE Healthcare no. 28-4083-47) according to the manufacturer's instructions. Serum was diluted 1:1 with 20 mM sodium phosphate and binding buffer (pH 7.0) and eluted with 0.1 M glycine-HCl (pH 2.7), and the pH was neutralized with 0.1 M glycine-HCl (pH 2.7). The eluted antibodies were then concentrated using an Amicon Ultra

0.5 centrifugal unit (Merck no. UFC500308) by centrifuging at 14,000 RCF for 30 min at 4°C and then washing the antibodies with 400 µl of PBS twice. The protein concentration was then quantified on a NanoDrop spectrophotometer at 280 nm using the extinction coefficients for IgG.

Testing CD200 expression on DFT cells that overexpress CD200R1

A total of 50,000 DFT cells per well were aliquoted into U-bottom 96-well plates and washed with 200 µl of cold FACS buffer. Purified polyclonal anti-CD200 was diluted to 2.5 µg/ml in cold FACS buffer, and the cells in appropriate wells were resuspend in 100 µl per well (0.25 µg per well) diluted antibody; wells that did not receive antibody were resuspended in 100 µl of FACS buffer. The cells were incubated on ice for 20 min and then washed with 200 µl of FACS buffer. While incubating, anti-mouse IgG AF647 was diluted to 1 µg/ml in cold FACS buffer and then used to resuspend cells in the appropriate wells. The plates were incubated on ice for 20 min and then washed with 100 µl of cold FACS buffer. The cells were then resuspended in 200 µl of FACS fix and incubated on a rocking platform at room temperature for 15 min. The cells were then centrifuged 500 RCF for 3 min at 4°C, resuspended in 200 µl of FACS buffer, and stored at 4°C until they were analyzed on a FACSCanto II ($N = 2$ per treatment) (Fig. 5E).

Isolation of devil PBMCs

Blood collection from Tasmanian devils was approved by the University of Tasmania Animal Ethics Committee (permit no. A0014599) and the Tasmanian Department of Primary Industries, Parks, Water and Environment. Blood was collected from the jugular vein and stored in EDTA tubes for transport to the laboratory. Blood was processed within 3 hours by diluting 1:1 with serum-free RPMI and then layering onto Histopaque (Sigma-Aldrich no. 10771) before centrifuging at 400 RCF for 30 min. The interface containing the PBMCs was then collected using a transfer pipette, diluted with 50 ml of serum-free RPMI, and centrifuged for 5 min at 500 RCF. Cells were washed with again with cRF10 and then either used fresh or stored at −80°C until further use.

Detecting DFT2 cells in PBMC using CD200

Frozen devil PBMC was thawed and cultured in cRF10 at 35°C with 5% CO_2 for 2 hours; cells were then washed in FACS buffer and counted, and 3×10^5 PBMCs were used per sample. DFT2.JV cells were removed from culture flasks and counted, and 2×10^5 cells were used per sample. Samples were incubated with 50 µl of normal goat serum (Thermo Fisher Scientific, catalog no. 01-6201) diluted 1:200 in FACS buffer for 15 min at 4°C, and 50 µl of anti-CD200 serum diluted 1:100 was added (1:200 final) for 30 min at 4°C. Cells were then washed two times and stained with 50 µl of anti-mouse IgG AF647 diluted to 1 µg/ml in FACS buffer for 30 min at 4°C. The cells were then washed two times, stained with DAPI (Sigma-Aldrich, catalog no. D9542) to identify live cells, and analyzed on the BD FACSCanto II. PBMC and DFT cells were run separately, and then PBMC and DFT2 were mixed at a ratio of 10:1 by volume for the combined samples ($N = 1$ per treatment) (fig. S4A). The experiment was repeated ($N = 1$ per treatment), except that PBMCs and DFT cells were mixed at a 5:1 ratio (fig. S4B).

Staining of DFT cells in devil whole blood

DFT1.C5065 and DFT2.JV cells were labeled with 5 µM CTV and cultured for 3 days at 37°C. On the day of the assays, peripheral blood from one devil was collected and stored at ambient temperature for less than 3 hours. One hundred microliters of whole blood was aliquoted into 15-ml tubes and stored at ambient temperature while DFT cells were prepared. The media on CTV-labeled DFT cells were decanted, and the cells were detached from the flask by incubating in 2.5 ml of TrypLE Select for 5 min at 37°C. The cells were washed with cRF10, resuspended in cRF10, and counted. DFT cells were then diluted to 1×10^4 cells/ml in cRF10, and 100 µl was aliquoted into appropriate 15-ml tubes containing 100 µl of whole blood. One microliter of purified anti-CD200 (0.5 µg per tube) was diluted into the appropriate tubes and incubated for 15 min at ambient temperature. Next, anti-mouse IgG AF647 (0.5 µg per tube) was added to each tube. Note: 0.5 µl (0.5 µg) of concentrated secondary antibody was accidentally added directly to the tube for the data shown in the top row, middle column of fig. S5A; for all other tubes, the secondary antibody was diluted 1:20 in PBS and 10 µl was added to each tube. The cells were then incubated for 15 min at ambient temperature. The cells were then diluted in 1 ml of ammonium chloride RBC lysis buffer [150 mM NH_4Cl, 10 mM $KHCO_3$, and 0.1 mM EDTA disodium (Na_2-$2H_2O$)] and mixed immediately gently pipetting five times. The cells were incubated at ambient temperature for 10 min, then diluted with 5 ml of PBS, and centrifuged 500 RCF for 3 min. Some tubes contained residual RBCs, so the pellet was vigorously resuspended in 5 ml of RBC lysis buffer, incubated for 5 min, diluted with 5 ml of cold FACS buffer, and centrifuged 500 RCF for 3 min. The cells were then resuspended in 250 µl of FACS buffer and stored on ice until analysis on a Beckman Coulter MoFlo Astrios ($N = 1$ per treatment). Data were analyzed in FCS Express version 6 (fig. S5).

The experiment above was repeated with the following modifications. DFT cells were labeled with 5 µM CFSE and incubated for 2 days at 37°C. On the day of the assays, fresh blood was collected from two devils. Purified anti-CD200 and NMS were labeled with Zenon mouse IgG AF647 (Thermo Fisher Scientific no. Z25008) and blocked with the Zenon blocking agent. A total of 1×10^4 CFSE-labeled DFT cells were diluted directly into 100 µl of whole blood in 15-ml tubes, and 12 µl (2-µl antibody, 5-µl labeling agent, and 5-µl blocking agent) of Zenon AF647–labeled purified NMS or anti-CD200 was added directly to the cells. The cells were incubated for 30 min at ambient temperature. The cells were then gently resuspended in 2.5 ml of RBC lysis buffer and incubated for 10 min at ambient temperature. The cells were diluted with 10 ml of PBS and centrifuged 500 RCF for 3 min. The cells were resuspended in 1.5 ml of RBC lysis buffer and incubated for another 10 min to lyse residual RBCs. The tubes were then resuspended in 9 ml of cRF10 and centrifuged 500 RCF for 3 min. The cells were resuspended in 350 µl of cold FACS buffer containing DAPI (200 ng/ml) and stored on ice until analysis on a Beckman Coulter MoFlo Astrios ($N = 1$ per treatment for $n = 2$ devils) (Fig. 6, A to D).

Construction of anti-human PD-L1 nanobody

The anti-human PD-L1 nanobody (KN035) (*24*) protein sequence was reverse-translated and as a double-stranded DNA gBlock (Integrated DNA Technologies) (table S5). The sequence was modified to include DNA extension that overlaps FAST vectors. The signal peptide from hamster IL-2 (also in pAF92) was added to the nanobody to increase secretion efficiency in CHO cells. The gBlock was inserted into a NotI-HF– and Sma I–digested mCitrine FAST vector with NEB HiFi DNA Assembly Master Mix (NEB no. E2621). Transformation, purification of plasmid DNA, and sequencing were performed as described above.

ExpiCHO transfection for nanobody production

ExpiCHO cells (Thermo Fisher Scientific no. A29127) for high-yield protein production were maintained at 37°C with 8% CO_2 with constant shaking at 200 rpm in ExpiCHO Stable Production Medium (SPM) (Thermo Fisher Scientific no. A3711001). ExpiCHO cells were added to a six-well plate at 3×10^5 cells per well in ExpiCHO SPM and cultured overnight. The next day, 2-μg plasmid DNA was added to 100 μl of PBS in a microcentrifuge tube. PEI was diluted to 60 μg/ml in PBS and incubated at room temperature for 5 min. Diluted plasmid DNA was added to 100 μl of PEI solution to achieve a 3:1 PEI:DNA ratio and incubated at room temperature for 15 min. During this time, ExpiCHO cells were transferred to 15-ml centrifuge tubes, washed with PBS at 300*g* for min, resuspended in 3-ml OptiPRO serum-free media (Thermo Fisher Scientific no. 12309019), and returned to the six-well plate. The PEI:DNA solution was then added directly to cells and incubated overnight. The next day, plates were inspected for fluorescence, and the media were removed and replaced with ExpiCHO SPM supplemented with hygromycin (1 mg/ml). Media were changed every second day until selection was complete. Once selection was complete, the cells were moved to 50-ml TPP TubeSpin bioreactor tubes (Sigma-Aldrich no. Z761028) and maintained at 4×10^6 to 6×10^6 cells/ml in ExpiCHO SPM with hygromycin (0.2 mg/ml). Supernatant was collected 2 weeks after transfection and stored at 4°C.

Staining CHO cells with PD-L1 nanobody in supernatant

CHO cells expressing either human PD-L1 or human CD80 fused to miRFP670 (table S3) were plated at 100,000 cells per well into a U-bottom 96-well plate and centrifuged at 300*g* for 5 min, and the supernatant was discarded. Two hundred–microliter supernatant containing secreted PD-L1 nanobody was added to CHO cell lines either neat or diluted in 1:10 and 1:100 in FACS buffer. Cells were incubated at 4°C for 30 min before being washed in FACS buffer for analysis on a Beckman Coulter FACSCanto II (Fig. 6F).

SUPPLEMENTARY MATERIALS

Supplementary material for this article is available at http://advances.sciencemag.org/cgi/content/full/6/27/eaba5031/DC1

View/request a protocol for this paper from *Bio-protocol*.

REFERENCES AND NOTES

1. T. A. F. Albuquerque, L. D. do Val, A. Doherty, J. P. de Magalhães, From humans to hydra: Patterns of cancer across the tree of life. *Biol. Rev. Camb. Philos. Soc.* **93**, 1715–1734 (2018).
2. M. Effron, L. Griner, K. Benirschke, Nature and rate of neoplasia found in captive wild mammals, birds, and reptiles at necropsy. *J. Natl. Cancer Inst.* **59**, 185–198 (1977).
3. W. A. Priester, N. Mantel, Occurrence of tumors in domestic animals. Data from 12 United States and Canadian colleges of veterinary medicine. *J. Natl. Cancer Inst.* **47**, 1333–1344 (1971).
4. N. Howlader, A. M. Noone, M. Krapcho, D. Miller, A. Brest, M. Yu, J. Ruhl, Z. Tatalovich, A. Mariotto, D. R. Lewis, H. S. Feuer, K. A. Cronin, *SEER Cancer Statistics Review, 1975–2016* (National Cancer Institute, 2016).
5. L. A. Griner, Neoplasms in Tasmanian devils (Sarcophilus harrisii). *J. Natl. Cancer Inst.* **62**, 589–595 (1979).
6. V. F. Pang, P.-H. Chang, F.-I. Wang, S.-C. Chin, C.-R. Jeng, C.-H. Chin, C.-R. Jeng, C.-H. Liu, P.-Y. Chu, Y.-X. Zhuo, Spontaneous neoplasms in zoo mammals, birds, and reptiles in Taiwan - A 10-year survey. *Anim. Biol.* **62**, 95–110 (2012).
7. S. J. Peck, S. A. Michael, G. Knowles, A. Davis, D. Pemberton, Causes of mortality and severe morbidity requiring euthanasia in captive Tasmanian devils (*Sarcophilus harrisii*) in Tasmania. *Aust. Vet. J.* **97**, 89–92 (2019).
8. A.-M. Pearse, K. Swift, Allograft theory: Transmission of devil facial-tumour disease. *Nature* **439**, 549 (2006).
9. R. J. Pye, D. Pemberton, C. Tovar, J. M. C. Tubio, K. A. Dun, S. Fox, J. Darby, D. Hayes, G. W. Knowles, A. Kreiss, H. V. T. Siddle, K. Swift, A. B. Lyons, E. P. Murchison, G. M. Woods, A second transmissible cancer in Tasmanian devils. *Proc. Natl. Acad. Sci. U.S.A.* **113**, 374–379 (2016).
10. C. Murgia, J. K. Pritchard, S. Y. Kim, A. Fassati, R. A. Weiss, Clonal origin and evolution of a transmissible cancer. *Cell* **126**, 477–487 (2006).
11. J. M. Fleming, K. E. Creevy, D. E. L. Promislow, Mortality in North American dogs from 1984 to 2004: An investigation into age-, size-, and breed-related causes of death. *J. Vet. Intern. Med.* **25**, 187–198 (2011).
12. B. T. Lazenby, M. W. Tobler, W. E. Brown, C. E. Hawkins, G. J. Hocking, F. Hume, S. Huxtable, P. Iles, M. E. Jones, C. Lawrence, S. Thalmann, P. Wise, H. Williams, S. Fox, D. Pemberton, Density trends and demographic signals uncover the long-term impact of transmissible cancer in Tasmanian devils. *J. Appl. Ecol.* **55**, 1368–1379 (2018).
13. S. James, G. Jennings, Y. M. Kwon, M. Stammnitz, A. Fraik, A. Storfer, S. Comte, D. Pemberton, S. Fox, B. Brown, R. Pye, G. Woods, B. Lyons, P. A. Hohenlohe, H. M. Callum, H. Siddle, F. Thomas, B. Ujvari, E. P. Murchison, M. Jones, R. Hamede, Tracing the rise of malignant cell lines: distribution, epidemiology and evolutionary interactions of two transmissible cancers in Tasmanian devils. *Evol. Appl.* **12**, 1772–1780 (2019).
14. H. V. Siddle, A. Kreiss, C. Tovar, C. K. Yuen, Y. Cheng, K. Belov, K. Swift, A.-M. Pearse, R. Hamede, M. E. Jones, K. Skjødt, G. M. Woods, J. Kaufman, Reversible epigenetic down-regulation of MHC molecules by devil facial tumour disease illustrates immune escape by a contagious cancer. *Proc. Natl. Acad. Sci. U.S.A.* **110**, 5103–5108 (2013).
15. A. Caldwell, R. Coleby, C. Tovar, M. R. Stammnitz, Y. M. Kwon, R. S. Owen, M. Tringides, E. P. Murchison, K. Skjødt, G. J. Thomas, J. Kaufman, T. Elliott, G. M. Woods, H. V. Siddle, The newly-arisen devil facial tumour disease 2 (DFT2) reveals a mechanism for the emergence of a contagious cancer. *eLife* **7**, e35314 (2018).
16. M. R. Stammnitz, T. H. H. Coorens, K. C. Gori, D. Hayes, B. Fu, J. Wang, D. E. Martin-Herranz, L. B. Alexandrov, A. Baez-Ortega, S. Barthorpe, A. Beck, F. Giordano, G. W. Knowles, Y. M. Kwon, G. Hall, S. Price, R. J. Pye, J. M. C. Tubio, H. V. T. Siddle, S. S. Sohal, G. M. Woods, U. M. Dermott, F. Yang, M. J. Garnett, Z. Ning, E. P. Murchison, The origins and vulnerabilities of two transmissible cancers in tasmanian devils. *Cancer Cell* **33**, 607–619.e15 (2018).
17. A. S. Flies, A. B. Lyons, L. M. Corcoran, A. T. Papenfuss, J. M. Murphy, G. W. Knowles, G. M. Woods, J. D. Hayball, PD-L1 is not constitutively expressed on Tasmanian devil facial tumor cells but is strongly upregulated in response to IFN-γ and can be expressed in the tumor microenvironment. *Front. Immunol.* **7**, 581 (2016).
18. C. E. B. Ong, A. B. Lyons, G. M. Woods, A. S. Flies, Inducible IFN-γ expression for MHC-I upregulation in devil facial tumor cells. *Front. Immunol.* **9**, 3117 (2018).
19. A. S. Flies, N. B. Blackburn, A. B. Lyons, J. D. Hayball, G. M. Woods, Comparative analysis of immune checkpoint molecules and their potential role in the transmissible Tasmanian devil facial tumor disease. *Front. Immunol.* **8**, 513 (2017).
20. A. S. Flies, E. J. Flies, S. Fox, A. Gilbert, S. R. Johnson, G.-S. Liu, A. B. Lyons, A. L. Patchett, D. Pemberton, R. J. Pye, An oral bait vaccination approach for the Tasmanian devil facial tumor diseases. *Expert Rev. Vaccines* , 1–10 (2020).
21. N. C. Shaner, R. E. Campbell, P. A. Steinbach, B. N. G. Giepmans, A. E. Palmer, R. Y. Tsien, Improved monomeric red, orange and yellow fluorescent proteins derived from *Discosoma* sp. red fluorescent protein. *Nat. Biotechnol.* **22**, 1567–1572 (2004).
22. H. J. Cha, N. N. Dalal, W. E. Bentley, Secretion of human interleukin-2 fused with green fluorescent protein in recombinant *pichia pastoris*. *Appl. Biochem. Biotechnol.* **126**, 1–11 (2005).
23. T. Duellman, J. Burnett, J. Yang, Quantitation of secreted proteins using mCherry fusion constructs and a fluorescent microplate reader. *Anal. Biochem.* **473**, 34–40 (2015).
24. F. Zhang, H. Wei, X. Wang, Y. Bai, P. Wang, J. Wu, X. Jiang, Y. Wang, H. Cai, T. Xu, A. Zhou, Structural basis of a novel PD-L1 nanobody for immune checkpoint blockade. *Cell Discov.* **3**, 17004 (2017).
25. A. L. Patchett, R. Wilson, J. C. Charlesworth, L. M. Corcoran, A. T. Papenfuss, B. A. Lyons, G. M. Woods, C. Tovar, Transcriptome and proteome profiling reveals stress-induced expression signatures of imiquimod-treated Tasmanian devil facial tumor disease (DFTD) cells. *Oncotarget* **9**, 15895–15914 (2018).
26. A. L. Patchett, T. H. H. Coorens, J. Darby, R. Wilson, M. J. McKay, K. S. Kamath, A. Rubin, M. Wakefield, L. Mcintosh, S. Mangiola, R. J. Pye, A. S. Flies, L. M. Corcoran, A. B. Lyons, G. M. Woods, E. P. Murchison, A. T. Papenfuss, C. Tovar, Two of a kind: Transmissible Schwann cell cancers in the endangered Tasmanian devil (*Sarcophilus harrisii*). *Cell. Mol. Life Sci.* 1847–1858 (2020).
27. O. S. Qureshi, Y. Zheng, K. Nakamura, K. Attridge, C. Manzotti, E. M. Schmidt, J. Baker, L. E. Jeffery, S. Kaur, Z. Briggs, T. Z. Hou, C. E. Futter, G. Anderson, L. S. K. Walker, D. M. Sansom, Trans-endocytosis of CD80 and CD86: A molecular basis for the cell extrinsic function of CTLA-4. *Science* **332**, 600–603 (2011).
28. A. L. Patchett, R. Latham, K. H. Brettingham-Moore, C. Tovar, A. B. Lyons, G. M. Woods, Toll-like receptor signaling is functional in immune cells of the endangered Tasmanian devil. *Dev. Comp. Immunol.* **53**, 123–133 (2015).
29. J. E. Love, K. Thompson, M. R. Kilgore, M. Westerhoff, C. E. Murphy, A. Papanicolau-Sengos, K. A. McCormick, V. Shankaran, N. Vandeven, F. Miller, A. Blom, P. T. Nghiem, S. J. Kussick, CD200 expression in neuroendocrine neoplasms. *Am. J. Clin. Pathol.* **148**, 236–242 (2017).

30. E. P. Murchison, C. Tovar, A. Hsu, H. S. Bender, P. Kheradpour, C. A. Rebbeck, D. Obendorf, C. Conlan, M. Bahlo, C. A. Blizzard, S. Pyecroft, A. Kreiss, M. Kellis, A. Stark, T. T. Harkins, J. A. M. Graves, G. M. Woods, G. J. Hannon, A. T. Papenfuss, The Tasmanian devil transcriptome reveals schwann cell origins of a clonally transmissible cancer. *Science* **327**, 84–87 (2010).
31. D. Sugiura, T. Maruhashi, I.-m. Okazaki, K. Shimizu, T. K. Maeda, T. Takemoto, T. Okazak, Restriction of PD-1 function by *cis* -PD-L1/CD80 interactions is required for optimal T cell responses. *Science* **364**, 558–566 (2019).
32. P. Challagundla, L. J. Medeiros, R. Kanagal-Shamanna, R. N. Miranda, J. L. Jorgensen, Differential expression of CD200 in B-cell neoplasms by flow cytometry can assist in diagnosis, subclassification, and bone marrow staging. *Am J Clin Pathol.* **142**, 837–844 (2014).
33. R. Loh, D. Hayes, A. Mahjoor, A. O'Hara, S. Pyecroft, S. Raidal, The immunohistochemical characterization of devil facial tumor disease (DFTD) in the Tasmanian Devil (*Sarcophilus harrisii*). *Vet. Pathol.* **43**, 896–903 (2006).
34. J. Wang, M. F. Sanmamed, I. Datar, T. T. Su, L. Ji, J. Sun, L. Chen, Y. Chen, G. Zhu, W. Yin, L. Zheng, T. Zhou, T. Badri, S. Yao, S. Zhu, A. Boto, M. Sznol, I. Melero, D. A. A. Vignali, K. Schalper, L. Chen, Fibrinogen-like protein 1 is a major immune inhibitory ligand of LAG-3. *Cell* **176**, 334–347.e12 (2018).
35. S. J. Coles, S. Man, R. Hills, E. C. Y. Wang, A. Burnett, R. L. Darley, A. Tonks, Over-Expression of CD200 In Acute Myeloid Leukemia Mediates the Expansion of Regulatory T-Lymphocytes and Directly Inhibits Natural Killer Cell Tumor Immunity. *Blood* **116**, 491 (2010).
36. R. M. Gorczynski, Z. Chen, I. Khatri, K. Yu, Graft-infiltrating cells expressing a CD200 transgene prolong allogeneic skin graft survival in association with local increases in Foxp3^{+}Treg and mast cells. *Transpl. Immunol.* **25**, 187–193 (2011).
37. J. Harding, K. Vintersten-Nagy, M. Shutova, H. Yang, J. K. Tang, M. Massumi, M. Izaidfar, Z. Izadifar, P. Zhang, C. J. Li, A. Nagy, Induction of long-term allogeneic cell acceptance and formation of immune privileged tissue in immunocompetent hosts. *bioRxiv*, 716571 (2019).
38. C. Tovar, R. J. Pye, A. Kreiss, Y. Cheng, G. K. Brown, J. Darby, R. C. Malley, H. V. T. Siddle, K. Skjødt, J. Kaufman, A. Silva, A. B. Morelli, A. T. Papenfuss, L. M. Corcoran, J. M. Murphy, M. J. Pearse, K. Belov, A. B. Lyons, G. M. Woods, Regression of devil facial tumour disease following immunotherapy in immunised Tasmanian devils. *Sci. Rep.* **7**, 43827 (2017).
39. R. Pye, A. Patchett, E. M. Lennan, R. Thomson, S. Carver, S. Fox, D. Pemberton, A. Kreiss, A. B. Morelli, A. Silva, M. J. Pearse, L. M. Corcoran, K. Belov, C. J. Hogg, G. M. Woods, A. B. Lyons, Immunization strategies producing a humoral IgG immune response against devil facial tumor disease in the majority of Tasmanian devils destined for wild release. *Front. Immunol.* **9**, 259 (2018).
40. M. R. Olin, E. Ampudia-Mesias, C. A. Pennell, A. Sarver, C. C. Chen, C. L. Moertel, M. A. Hunt, G. E. Pluhar, Treatment combining CD200 immune checkpoint inhibitor and tumor-lysate vaccination after surgery for pet dogs with high-grade glioma. *Cancers (Basel).* **11**, 137 (2019).
41. S. Zhang, J. H. Phillips, Identification of tyrosine residues crucial for CD200R-mediated inhibition of mast cell activation. *J. Leukoc. Biol.* **79**, 363–368 (2006).
42. D. Hatherley, S. M. Lea, S. Johnson, A. N. Barclay, Structures of CD200/CD200 receptor family and implications for topology, regulation, and evolution. *Structure* **21**, 820–832 (2013).
43. Z.-X. Luo, C.-X. Yuan, Q.-J. Meng, Q. Ji, A Jurassic eutherian mammal and divergence of marsupials and placentals. *Nature* **476**, 442–445 (2011).
44. K. K. Wong, I. Khatri, S. Shaha, D. E. Spaner, R. M. Gorczynski, The role of CD200 in immunity to B cell lymphoma. *J. Leukoc. Biol.* **88**, 361–372 (2010).
45. J. M. Alves, M. Carneiro, J. Y. Cheng, A. L. de Matos, M. M. Rahman, L. Loog, P. F. Campos, N. Wales, A. Eriksson, A. Manica, T. Strive, S. C. Graham, S. Afonso, D. J. Bell, L. Belmont, J. P. Day, S. J. Fuller, S. Marchandeau, W. J. Palmer, G. Queney, A. K. Surridge, F. G. Vieira, G. M. Fadden, R. Nielsen, M. T. P. Gilbert, P. J. Esteves, N. Ferrand, F. M. Jiggins, Parallel adaptation of rabbit populations to myxoma virus. *Science* , 1319–1326 (2019).
46. E. Kowarz, D. Löscher, R. Marschalek, Optimized Sleeping Beauty transposons rapidly generate stable transgenic cell lines. *Biotechnol. J.* **10**, 647–653 (2015).
47. L. Mátés, M. K. L. Chuah, E. Belay, B. Jerchow, N. Manoj, A. Acosta-Sanchez, D. P. Grzela, A. Schmitt, K. Becker, J. Matrai, L. Ma, E. Samara-Kuko, C. Gysemans, D. Pryputniewicz, C. Miskey, B. Fletcher, T. V. Driessche, Z. Ivics, Z. Izsvák, Molecular evolution of a novel hyperactive *Sleeping Beauty* transposase enables robust stable gene transfer in vertebrates. *Nat. Genet.* **41**, 753–761 (2009).
48. E. Gasteiger, C. Hoogland, A. Gattiker, S. Duvaud, M. R. Wilkins, R. D. Appel, A. Bairoch, in *The Proteomics Protocols Handbook*, J. M. Walker, Ed. (Humana Press, ed. 1, 2005), pp. 571–607.

Acknowledgments: We wish to thank G. Ralph for ongoing care of Tasmanian devils, the Bonorong Wildlife Sanctuary for providing access to Tasmanian devils, and R. Pye for providing care for devils and collecting blood samples. We would like to thank J. Hayball, C. Espejo, and G. Kalodimos for advice and assistance, M. Kingsley and N. Poudel for plasmid construction, N. Blackburn for bioinformatics assistance, L. Corcoran for the devil IgG plasmid, J. Murphy for a devil IL-15 plasmid, E. Flies for editing the manuscript, and K. Holekamp for comments on the manuscript. **Funding:** This study was funded by ARC DECRA grant no. DE180100484, ARC Linkage grant no. LP0989727, ARC Discovery grant no. DP130100715, Morris Animal Foundation Grant-in-Aid no. D14ZO-410, University of Tasmania Foundation Dr. Eric Guiler Tasmanian Devil Research Grant through funds raised by the Save the Tasmanian Devil Appeal (2013, 2015, 2017, 2018), and Entrepreneurs' Programme-Research Connections grant with Nexvet Australia Pty. Ltd. no. RC50680, Royal Hobart Hospital Research Foundation Incubator Grant no. F0026331. **Author contributions:** A.S.F. designed the study. A.D.L., A.L.P., A.S.F., C.E.B.O., P.R.L., and P.R.M. developed the technology. A.D.L., A.S.F., C.E.B.O., P.R.L., P.R.M., J.M.D., and T.L.P. performed the experiments. A.L.P. performed bioinformatic analyses. A.L.P., A.S.F., J.M.D., and P.R.L. created the figures. A.L.P., A.S.F., P.R.L., J.M.D., T.L.P., and G.M.W. analyzed the data. A.S.F. wrote the manuscript, and all authors edited the manuscript. **Competing interests:** The authors received funding from Nexvet Australia Pty. Ltd. for related studies. The authors declare that they have no other competing interests. **Data and materials availability:** The FAST base vectors pAF92.3 (no. 135929), pAF112.7 (no. 135920), pAF123.1 (no. 135921), pAF138.7 (no. 135923), pAF139.2 (no. 135924), pAF160.1 (no. 135925), pAF161.3 (no. 135926), pAF163.1 (no. 135927), pAF164.3 (no. 135928), and pAF197 (no. 135930) are available from Addgene (www.addgene.org/Andrew_S._Flies/). The plasmids used in the construction of new plasmids for this study can be provided by Addgene pending a completed material transfer agreement. Requests for the plasmids should be submitted to Addgene. All data needed to evaluate the conclusions in the paper are present in the paper and/or the Supplementary Materials. Additional data related to this paper may be requested from the authors. All experimental protocols and data are publicly available at https://rdp.utas.edu.au/metadata/1068adf9-9124-45c6-af79-40ee47e00c48. Protocols and experimental templates are available at WildImmunity.com/resources.

Submitted 9 December 2019
Accepted 20 April 2020
Published 1 July 2020
10.1126/sciadv.aba5031

Citation: A. S. Flies, J. M. Darby, P. R. Lennard, P. R. Murphy, C. E. B. Ong, T. L. Pinfold, A. De Luca, A. B. Lyons, G. M. Woods, A. L. Patchett, A novel system to map protein interactions reveals evolutionarily conserved immune evasion pathways on transmissible cancers. *Sci. Adv.* **6**, eaba5031 (2020).

ScienceAdvances

A novel system to map protein interactions reveals evolutionarily conserved immune evasion pathways on transmissible cancers

Andrew S. FliesJocelyn M. DarbyPatrick R. LennardPeter R. MurphyChrissie E. B. OngTerry L. PinfoldAlana De LucaA. Bruce LyonsGregory M. WoodsAmanda L. Patchett

Sci. Adv., 6 (27), eaba5031. • DOI: 10.1126/sciadv.aba5031

Science Advances (ISSN 2375-2548) is published by the American Association for the Advancement of Science. 1200 New York Avenue NW, Washington, DC 20005. The title *Science Advances* is a registered trademark of AAAS.